Classification
Physics Abstracts
47.55M — 05.60

Hydrodynamic dispersion on self-similar structures : a Laplace space renormalization group approach

Emmanuel Villermaux ([1]) and Daniel Schweich ([2])

([1]) Institut de mécanique de Grenoble (*), BP 53 X, 38041 Grenoble Cedex, France
([2]) Laboratoire des Sciences du Génie Chimique, CNRS, ENSIC, 1 rue Grandville, BP 451, 54001 Nancy Cedex, France

(*Received 18 March 1991, revised 9 November 1991, accepted 8 January 1992*)

Abstract. — A general method for calculating the properties of the Residence Time Distribution (RTD) of a fluid flowing though a self-similar network, with or without stagnation (trapping) effects, in the high Péclet number limit is developed. The renormalization procedure adopted yields the Laplace transform of the Residence Time Distribution and allows one to calculate its time moments. The incidence of the connectivity of the medium on dispersion is discussed. The fractal dimension does not appear explicitly in the dispersion properties of the network. Geometrical dispersion is shown to result from the difference of pathlengths offered to the fluid in the generating pattern of the network. The dispersion front is strongly non-Gaussian and presents several maxima (short circuits) in some extreme cases. An approximate expression for the dispersion front is derived when the distribution of pathlengths is narrow. In the latter situation, a dispersion coefficient can be defined, and it is characterised by two parameters, γ and $(1-f)\,t_m$, which represent respectively the intensity of the disorder (or the ability to mixing) related to geometric dispersion, and the characteristic hold-up time of a tracer particle in the stagnation phase supposed to occupy a fraction $(1-f)$ of the volume and to be uniformly distributed in the medium. We also discuss the conditions of moments convergence and the long time asymptotic form of the RTD.

Introduction.

Hydrodynamic dispersion is a classical topic of statistical physics and serves as a useful tool to improve the understanding of various phenomena such as traffic flow, mixing in chemical reactors, oil recovery, polluant transport and, generally speaking, the spreading of a tracer in a medium of complex and disordered structure.

As far as porous media are concerned, recent experimental and theoretical investigations have pointed out the basic mechanisms of hydrodynamic dispersion [1-3]. Two essential processes account for dispersion : first, the spatial fluctuations of the flow velocity field (i.e., geometric dispersion), and second, the possible trapping effects of the tracer in regions of the

(*) UMR 101.

porous medium where the fluid is motionless (dead ends). The latter process involves molecular diffusive effects or/and adsorption effects on the solid matrix.

Strongly disordered media are known to be often locally self-similar (fractal) : the regions offered to fluid flow in a porous medium have been shown to be percolating clusters [4]. It is thus worth studying hydrodynamic dispersion (or directed dispersion by contrast with free Brownian motion) on self-similar structures. In this view, a porous medium might be modelled by a series of fractal regions. We investigate the dispersion properties of each fractal region, and of the series as a whole. Our study starts with an original formulation of the microscopic process of mixing consistent with previous approaches [3, 11] and also [15] in the context of alternative current response of inhomogeneous materials, which is convenient for recurrent computations on self-similar structures.

1. The local convection approximation.

Consider a disordered medium with a linear size L (Fig. 1) crossed by a fluid of average drift velocity U. The average length ℓ of a path through the medium of extension L is given by the porosity ε as $\ell = L/\varepsilon$. The average transit time is $\tau_c = \ell/u = L/U$ where $u = U/\varepsilon$ is the interstitial velocity of the fluid. Finally, the molecular diffusion time over the path ℓ is $\tau_d = \ell^2/D_m$. The relative intensity of molecular diffusion to the convective effects on the path ℓ is given by the ratio

$$\frac{\tau_d}{\tau_c} = \frac{U\ell^2}{LD_m} = \frac{L}{\delta\varepsilon^2}\mathrm{Pe}\,, \quad \mathrm{Pe} = \frac{U\delta}{D_m}$$

where δ is the size of the interstices. It is clear that in the high Péclet number (Pe) limit and in absence of a stagnant phase, molecular diffusive effects are negligible. At the level of the pores between the particles of the porous medium, the local mass balance equation for an inert tracer is

$$\left[\frac{\partial C}{\partial t} + u\frac{\partial C}{\partial x}\right]_i = 0 \tag{1}$$

where u is the interstitial velocity, and x the local coordinate parallel to flow (Fig. 2). The brackets $[\ ]_i$ denote that the mass balance equation is formulated at the microscopic level, that means the smallest physical lengthscale of the problem. At the macroscopic scale, the mass balance equation becomes

$$\frac{\partial C}{\partial t} + U\frac{\partial C}{\partial x} = D_{\parallel}\frac{\partial^2 C}{\partial x^2} \tag{2}$$

where x is now the direction of the mean flow, and $D_{\parallel}$ the dispersion coefficient. Our goal is to relate this coefficient to the geometrical structure of the self-similar network and the possible stagnation effects.

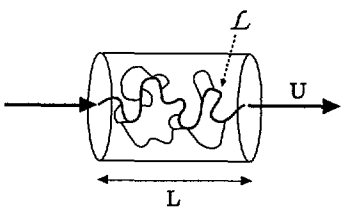

Fig. 1. — A porous medium of length L, crossed by a fluid at a mean velocity U. The average length of a tracer trajectory is ℓ.

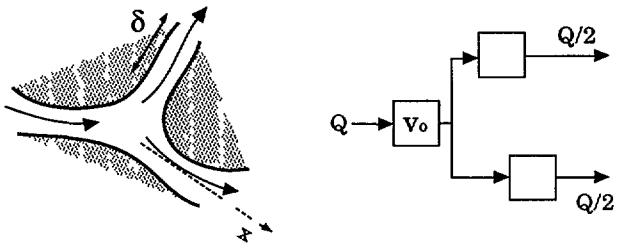

Fig. 2. — Left : typical pore connection in the actual medium. Right : the connection is accounted for by an element of the model network composed of microscopic units of volume v_0. The volume v_0 is such that $v_0 \sim \delta^3$, where δ is the size of the interstices. The flowrate Q in the incoming pore is distributed in the downstream pores with a partition ω_i, with $\sum_i \omega_i = 1$.

2. The transfer function formulation.

Consider a set of tracer particles entering a steady flow system. They may leave the system together or in a dispersed order. Following Danckwerts (1953) [5] (see also [2, 6, 7]), we denote by $E(t)$ the Residence Time Distribution (RTD). The fraction of fluid which resides in the flow system within t and $t + \mathrm{d}t$ is

$$E(t)\,\mathrm{d}t\,. \tag{3}$$

Assuming the tracer particles are instantaneously injected (i.e., Dirac δ injection) in the porous system, and letting $C_O(t)$ be the concentration of the tracer at the outlet of the system, one has

$$E(t)\,\mathrm{d}t = \frac{C_O(t)\,\mathrm{d}t}{\int_0^\infty C_O(t)\,\mathrm{d}t} \tag{4}$$

$E(t)$ is an intrinsic property of the system which depends only on its geometric features (convectivity of the pores, existence of stagnant zones), on its hydrodynamic state (turbulent or laminar), and, more generally, on its ability to mixing. When $C_I(t)$ is the concentration of tracer at the inlet of the system, then $C_O(t)$ is given by the convolution integral

$$C_O(t) = \int_0^t E(\tau)\,C_I(t-\tau)\,\mathrm{d}\tau\,. \tag{5}$$

Going to the Laplace domain, (5) becomes

$$G(s) = \int_0^\infty E(t)\,\mathrm{e}^{-st}\,\mathrm{d}t = \frac{C_O(s)}{C_I(s)} \tag{6}$$

where s is the Laplace parameter. The Laplace transform $G(s)$ of $E(t)$ is usually called the transfer function of the flow system. The moments of the distribution $E(t)$ are simply related to $G(s)$ by

$$\mu_k = \int_0^\infty t^k E(t)\,\mathrm{d}t = (-1)^k \left[\frac{\partial^k}{\partial s^k} G(s)\right]_{s=0} \tag{7}$$

Equation (7) means that $G(s)$ is the moment generating function of $E(t)$. According to (7), the variance of the residence time distribution is

$$\sigma_t^2 = \left[\frac{\partial^2}{\partial s^2} G(s)\right]_{s=0} - \left(-\left[\frac{\partial}{\partial s} G(s)\right]_{s=0}\right)^2 \tag{8a}$$

When there are no stagnation (trapping) effect we will write

$$\sigma_t^2 = (2\gamma - 1)\,\mu_1^2 . \tag{8b}$$

Parameter γ will be used to compare the variance of the actual RTD with reference RTDs.

In what follows, we will describe an arbitrary flow pattern by a suitable network of elementary flow units of known RTD $E_0(t)$. A simple and idealized schematic example is given in figure 2. Two special and idealized elementary flow systems will be of interest :

• Perfect plug flow where all the particles have the same residence time in the system, and where no mixing occurs

$$E_0(t) = \delta(t - \tau_0), \qquad \mu_1 = \tau_0, \qquad \gamma = 1/2 \tag{9}$$

which gives

$$G_0(s) = e^{-s\tau_0} \tag{10}$$

The RTD (9) is the solution for equation (1) when τ_0 is the convection time in the interstice.

• The perfect mixing cell where the outlet stream has the same composition as the bulk of the cell. This is the situation of maximal mixing, and

$$E_0(t) = \frac{1}{\tau_0} e^{-t/\tau_0}, \qquad \mu_1 = \tau_0, \qquad \gamma = 1 \tag{11}$$

which gives

$$G_0(s) = \frac{1}{1 + \tau_0 s} \tag{12}$$

Equation (11) comes from a mass balance for the tracer over the cell. Let v_0 be the volume of the cell, and Q the feed flow rate ; the mass balance equation is

$$v_0 \frac{dC_O}{dt} = Q(C_I - C_O), \qquad \tau_0 = v_0/Q . \tag{13}$$

Which is equivalent to equation (1) at the scale of the cell when a first order approximation is used for the spatial derivative.

With these basic tools in hand, we can easily model the RTD of the whole network of elementary units (either plug flow or mixing cell) using the following rules resulting from equations (4) and (6) :

— the transfer function of units in series is the product of the transfer functions of the units ;

— at the nodes of the network, the transfer functions are combined according to Kirschoff's law.

We will essentially use the perfect mixing cell as the basic flow unit because it allows one to simply model various mixing states. Letting

$$g_0(\tau_0 s) = \frac{1}{1 + \tau_0 s} \tag{14}$$

be the elementary transfer function, the zero mixing state is obtained when there is only one path (a unique residence time) in the network of mixing cells. It is, for instance, realized by an infinite series of vanishingly small and identical microscopic mixing cells (Fig. 3a) with a total volume V. Applying the first rule given above and using (14), the overall transfer function for the series is found to be

$$\Gamma_N(s) = [g_0(\tau_0 s)]^N, \quad \tau_0 = \frac{\tau}{N}, \quad \tau = \frac{V}{Q}, \quad \gamma = \frac{N+1}{2N} \tag{15}$$

In the limit of vanishingly small mixing cells, (14) gives

$$G(s) = \Gamma(s) = \lim_{N \to \infty} \left(\frac{1}{1 + \tau s/N} \right)^N = e^{-s\tau} \tag{16}$$

We recover here the well-known result that a volume V divided into an infinite series of well-stirred zones is equivalent to a plug flow, that is, to a non dispersive system [6].

The other already mentioned limit is that of perfectly well mixed flow. This limit can be obtained if we consider a system made of microscopic mixing cells placed in parallel (Fig. 3b). The overall transfer function is then

$$G(s) = g_0(\tau_0 s) = \frac{1}{1 + \tau s}, \quad \tau_0 = \frac{v_0}{Q/N} = \frac{V/N}{Q/N} = \frac{V}{Q} = \tau . \tag{17}$$

Intermediate mixing, or dispersion states can be modeled with the concept of continuous-time random walk [13, 14] with an exponential waiting time distribution at each step. Assuming that we are interested in the RTD at step N, and that τ_0 is the time constant of the waiting time distribution, the RTD is $\Gamma_N(s)$. Consequently, N mixing cells in series, with finite N, can account for a dispersed plug flow [2, 6, 7, 9], at least in the high Péclet number limit. This property will be used later to compare the RTD of a self-similar network with the RTD of a standard dispersed plug flow represented by $\Gamma_N(s)$.

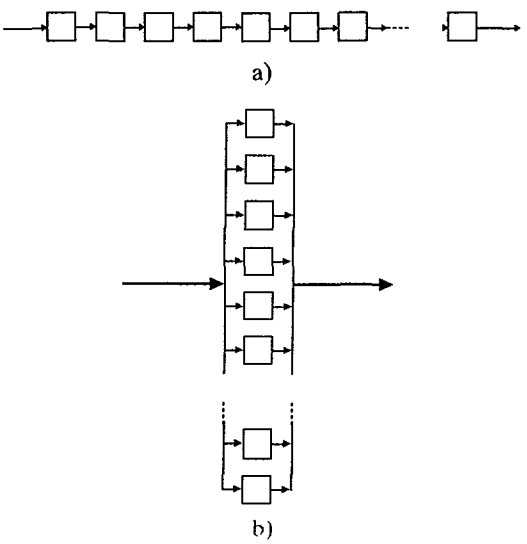

Fig. 3. — The two limit bounds of mixedness. a) Linear series of mixing cells, which yields no mixing in the infinite limit. b) Mixing cells in parallel leading to a perfectly mixed macroscopic volume.

We now focus our attention on strongly disordered media bearing self-similar flow-paths regions. The existence of a stagnant phase in the medium requires a modification of the microscopic transfer function $g_0(\tau_0 s)$, therefore we will split the study into two successive sections in order to clearly distinguish between geometric and trapping effects on dispersion.

3. Geometrical dispersion.

Consider the recurrent structure of figure 4. The network is fed by a flowrate Q of carrier fluid, and has a total volume V. The generating flow pattern ($n = 1$, Fig. 4) is made of three mixing cells of transfer functions derived from $g_0(\tau_0 s)$ according to the partition of the flow rate between the parallel branches. In figure 4, only three generations of the constructions are illustrated. The procedure exposed below consists of computing the transfer function $g_n(\tau s)$ corresponding to n similar repetitions of the generating pattern. The passage to the limit $n \to \infty$ permits one, first to find $G(s)$, the transfer function of the limiting network, and second to obtain the time moments of $E(t)$ by an expansion of $G(s)$ about $s = 0$. In this limit, an elementary mixing cell represents an infinitesimal part of the whole volume V (precisely $V/3^n$), as requested by the local convective limit discussed in section I. We first focus on the first two moments, such that

$$G(s) = \lim_{n \to \infty} g_n(\tau s) = 1 - \mu_1 s + \frac{\mu_2}{2} s^2 + O(s^3) . \tag{18}$$

For the sake of simplicity, we further suppose that the flow rate is equally distributed in the downstream pores at each node of the network. For instance in figure 4, $n = 1$, the flow rate in the two parallel branches is $Q/2$. This corresponds to a kind of ergodicity assumption under which the tracer particle should spend a mean time proportional to the volume of each pore [3]. According to this assumption, the mean residence time in the branches at a given level should not depend on the flowrate partition, but only on the volume of the branches, and this condition is realized by the equipartition of Q. The case corresponding to a partition of the flowrate such that the pressure drop would be equal in each branch (that is $Q/3$ in the branch bearing two cells and $2\,Q/3$ in the other branch) as well as any other flowrate partition can be treated by the same method and the general results are exposed in the appendix. We will refer to this later.

Going back to the example of figure 4, we want now to express the transfer function of the n-th generation $g_n(\tau s)$ as a function of $g_{n-1}(\tau s)$ by a renormalization procedure. Assuming V is fixed, the total volume of the network at level $n - 1$ is one third of the volume at step n. As we calculate the transfer function g_n at each step with respect to the same total flow rate Q, the argument of g_n is $Vs/Q = \tau s$, whereas the argument of g_{n-1} is $(V/3)/(Q/2)\, s = 2\,\tau s/3$. A simple mass balance over the nodes of the network gives the recurrence relation related to the pattern of figure 4

$$g_n(\tau s) = \frac{1}{2} [g_{n-1}^2(2\,\tau s/3) + g_{n-1}(2\,\tau s/3)] \tag{19}$$

with the initial condition $g_0(\tau_0 s) = 1/(1 + \tau_0 s)$, $\tau = 3^n \tau_0$. A numerical inversion of g_n, giving the RTD $E_n(t)$ at various steps is shown in figure 5. $E_n(t)$ rapidly becomes stationary with respect to n, typically as n approaches 50. This suggests that $g_n(\tau s)$ reaches a limit which should be the solution for the fixed point equation obtained when deleting subscripts n and $n - 1$ in equation (19). Since, according to (7), the moments of $E_n(t)$ can be derived from $g_n(\tau s)$, equation (19) is also a recurrence equation for the

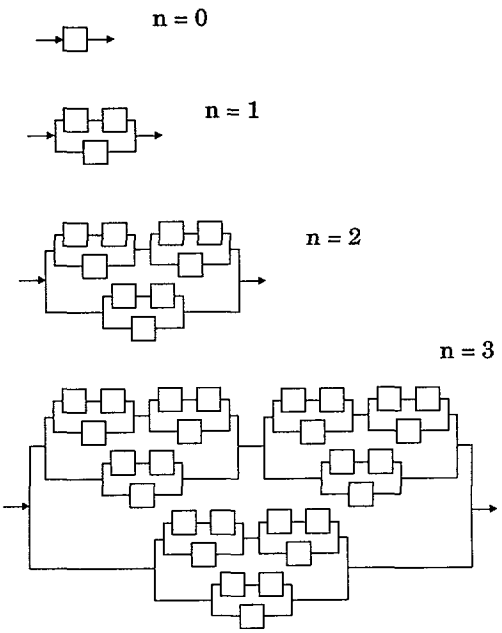

Fig. 4. — Three successive steps of construction of a self-similar network, starting from the elementary cell ($n = 0$) of transfer function g_0, and the generating pattern ($n = 1$).

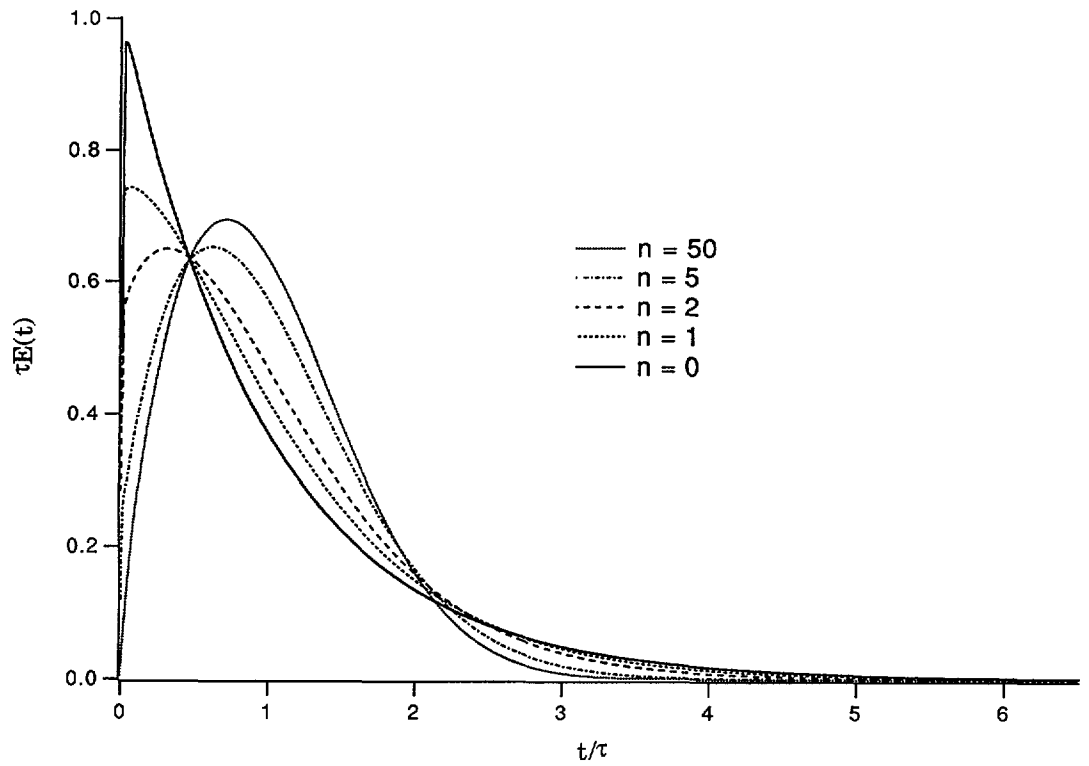

Fig. 5. — Evolution of the residence time distribution (dispersion front resulting from a Dirac pulse at the inlet of the network) according to the step of construction n of the self-similar network of figure 4.

moments. As explained in the appendix, the successive derivatives of (19) with respect to $x = \tau s$ provide a recurrence equation for each moment of order j, $\mu_{j,n}$, of $E_n(t)$.

We now assume that the generating pattern is made of several parallel branches, each of them being fed with a fraction ω_i of the total flowrate and containing k_i mixing cells (see Fig. 13 in the appendix). The mathematical derivations given in the appendix lead to the following results. The recurrence relationship is

$$G_n(s) = g_n(\tau s) = \sum_i \omega_i \left(g_{n-1}\left[\frac{\tau s}{k\omega_i} \right] \right)^{k_i} \tag{20a}$$

Provided that all the moments $\mu_{j,n}$ converge as n tends to infinity, the limiting transfer function $G(s)$ is the unique solution of the fixed point equation

$$G(s) = g(\tau s) = \sum_i \omega_i \left(g\left[\frac{\tau s}{k\omega_i} \right] \right)^{k_i} \tag{20b}$$

All the moments $\mu_{j,n}$ converge with n if and only if

$$C_j = \sum_i \frac{k_i}{k} \frac{1}{(k\omega_i)^{j-1}} < 1 , \qquad k = \sum_i k_i . \tag{21a}$$

Condition (21a) is fulfilled if and only if

$$k\omega_i > 1 . \tag{21b}$$

To understand qualitatively (21b), one may notice that $1/k\omega_i$ is the renormalizing factor of the mean residence time in a cell of branch i from generation n to generation $n+1$. This factor has to be less than unity otherwise the residence time in this branch would increase to infinity with n leading to an « accumulation zone » in the network, that is to a very broad final distribution $E(t)$ and to diverging moments. Note that when the flowrates are either equally distributed in all branches, or partitioned such that the pressure drop is the same in all branches, condition (21a) is always fulfilled (see appendix).

The recurrence relation for the moments gives, at order two, the expansion of $g_n(\tau s)$

$$g_n(\tau s) = 1 - \mu_{1,n} s + \frac{\mu_{2,n}}{2} s^2 + O(s^3) \tag{22}$$

with

$$\mu_{1,n} = \tau = V/Q . \tag{23}$$

Letting $\gamma_n = \mu_{2,n}/2\,\mu_{1,n}^2$, one obtains the relation (see appendix (Eq. (A16)))

$$\gamma_n = B + A\gamma_{n-1} , \quad A = C_2 = \sum_i \frac{k_i}{k^2\omega_i} , \quad B = \sum_i \frac{k_i(k_i-1)}{2k^2\omega_i} \tag{24}$$

$$\gamma_n = \frac{A^n g_0''(0)}{2} + B\frac{1-A^n}{1-A} \tag{25}$$

and, provided (21b) is fulfilled

$$\gamma = \lim_{n\to\infty} \gamma_n = \frac{B}{1-A} . \tag{26}$$

In the particular example of figure 4, $k_1 = 1$, $k_2 = 2$, $\omega_1 = \omega_2 = 0.5$. $A = 2/3$, $B = 2/9$ and $\gamma = 2/3$. Thus

$$G(s) = 1 - \tau s + \frac{2}{3}(\tau s)^2 + O(s^3) \tag{27}$$

is the exact expansion in s^2 of the transfer function of the self-similar network at infinite generation. With $\gamma = 2/3$, this network exhibits a dispersive behaviour which is intermediate between plug flow ($\gamma = 1/2$) and the macroscopic perfect mixing cell ($\gamma = 1$).

One can proceed in a similar manner with other types of generating patterns. Figure 6 shows some simple and typical cases, which define two distinct classes. Patterns leading to $1/2 < \gamma < 1$ present different pathlengths to the fluid. The possible paths of different lengths in the network at infinite generation imply a broad (most of the time irregular ; this point is discussed later) macroscopic distribution of pathlengths. The more the pathlengths in the generating pattern differ, the closer γ is to 1. Conversely, patterns which involve only one possible path give rise to only one macroscopic pathlength, that is to a unique residence time characteristic of plug flow ($\gamma = 1/2$).

When condition (21b) is fulfilled, the fixed point equation (20b) shows that the limiting transfer function $G(s)$ and its moments are independent of g_0. This is consistent with the fact that the local convective equation (1) can be modelled, in the differential limit ($\tau_0 \to 0$), by

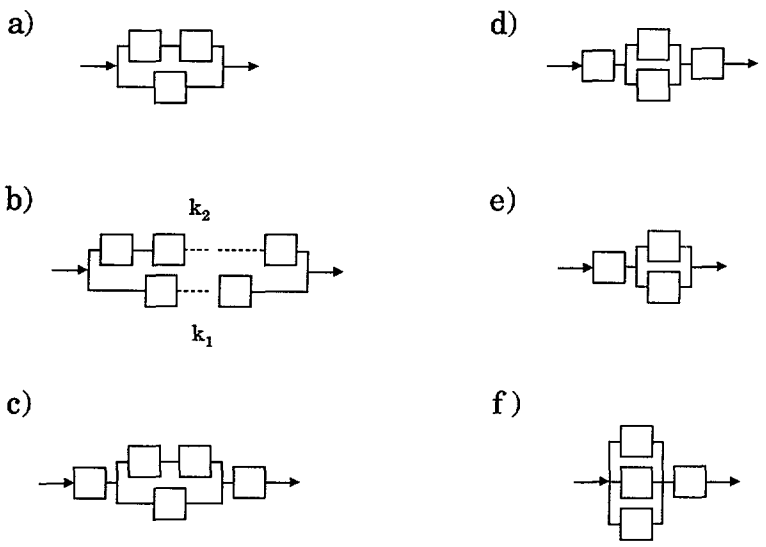

Fig. 6. — A few examples of generating patterns. Assuming equipartition of the flowrate in the branches, patterns a), b), c) present two paths of different lengths and lead to $1/2 < \gamma < 1$. Patterns d), e), f) exhibit a single pathlength and lead to $\gamma = 1/2$. The recurrence relations are :

a) $g_n(3^n \tau_0 s) = [g_{n-1}(3^{n-1} 2 \tau_0 s)^2 + g_{n-1}(3^{n-1} 2 \tau_0 s)]/2$; $\gamma = 2/3$;

b) $g_n((k_1 + k_2)^n \tau_0 s) = [g_{n-1}((k_1 + k_2)^{n-1} 2 \tau_0 s)^{k_1} + g_{n-1}((k_1 + k_2)^{n-1} 2 \tau_0 s)^{k_2}]/2$,
$2\gamma - 1 = (k_2 - k_1)^2/[(k_1 + k_2)(k_1 + k_2 - 2)]$;

c) $g_n(5^n \tau_0 s) = g_{n-1}(5^{n-1} \tau_0 s)^2 [g_{n-1}(5^{n-1} 2 \tau_0 s)^2 + g_{n-1}(5^{n-1} 2 \tau_0 s)]/2$; $\gamma = 9/17$;

d) $g_n(4^n \tau_0 s) = g_{n-1}(4^{n-1} \tau_0 s)^2 g_{n-1}(4^{n-1} 2 \tau_0 s)$; $\gamma = 1/2$;

e) $g_n(3^n \tau_0 s) = g_{n-1}(3^{n-1} \tau_0 s) g_{n-1}(3^{n-1} 2 \tau_0 s)$; $\gamma = 1/2$;

f) $g_n(4^n \tau_0 s) = g_{n-1}(4^{n-1} \tau_0 s) g_{n-1}(4^{n-1} 3 \tau_0 s)$; $\gamma = 1/2$.

any flow system with characteristic residence time τ_0. The fixed point equation can also be used for calculating the limiting moments. In the case of figure 4, one obtains

$$G(s) = g(\tau s) = \frac{1}{2}\left[g^2\left(\frac{2}{3}\tau s\right) + g\left(\frac{2}{3}\tau s\right)\right]. \tag{28}$$

Then, using (7) and $\mu_1 = \tau$, successive derivatives with respect to s give $\mu_2 = (4/3)\,\mu_1^2$, $\mu_3 = (32/15)\,\mu_1^3$, $\mu_4 = (3\,328/855)\,\mu_1^4$.. The fixed point equation can be found for any generating pattern as soon as the recurrence relation is derived, and it allows one, as an alternative method to that presented in the appendix, to calculate the complete series of time-moments by an expansion of $G(s)$ in powers of s by a recurrent method. However, let us mention that when condition (21b) is not fulfilled, the existence and uniqueness of the fixed point solution is not demonstrated. Using the fixed point equation to obtain the moments can lead to erroneous results in that case.

To compare the dispersion state resulting from the self-similarity with a standard dispersed plug flow, we match the variances of $G(s)$ and of $\Gamma_N(s)$ (see Eq. (15)) to obtain

$$N = \frac{1}{2\gamma - 1}. \tag{29}$$

For $\gamma = 2/3$, the RTD of the self-similar network of figure 4 at infinite generation is compared with the RTD of a series of $N = 3$ mixing cells in figure 7. This comparison shows that the RTD of some self-similar networks can be close to the RTD of mixing cells in series, or alternatively, of a standard dispersed plug flow even though N is low (or γ close to 1).

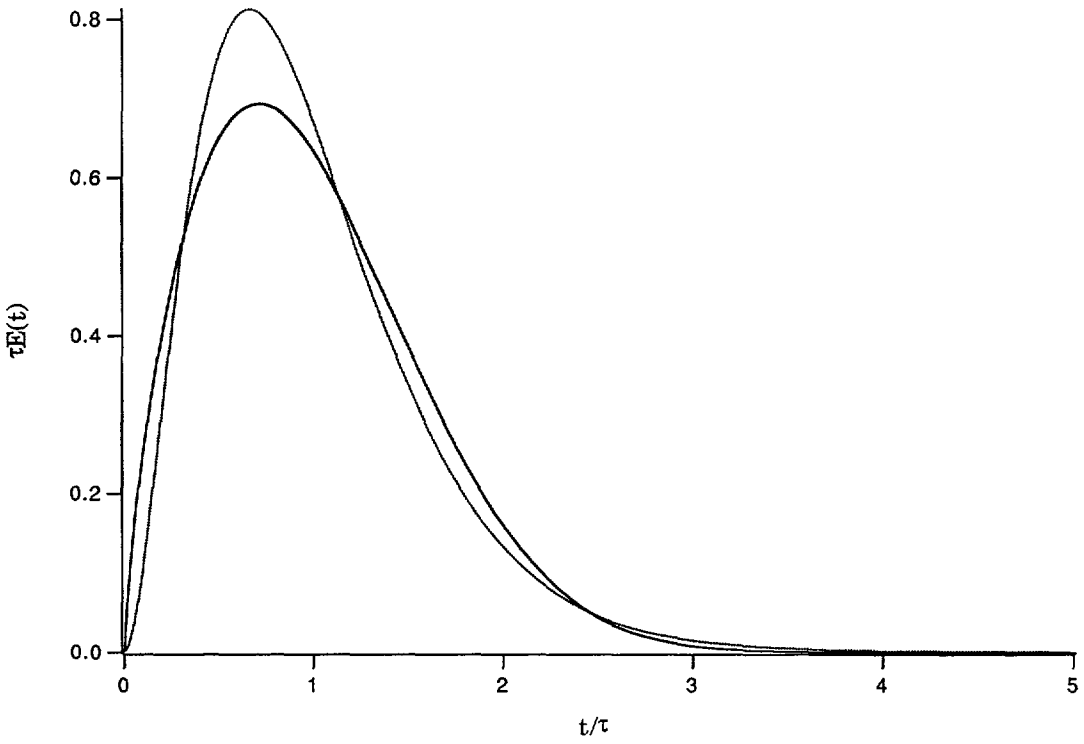

Fig. 7. — Solid line : RTD of the network of figure 4 at infinite generation ($n = 50$). Dotted line : RTD of $N = 3$ mixing cells in series.

However, this is not a general rule. Considering the generating pattern made of two parallel channels containing k_1 and k_2 microscopic cells respectively and fed with equal flow rates (see Fig. 6b), one finds

$$g_n[(k_1 + k_2)^n \tau_0 s] = \frac{1}{2}\left\{g_{n-1}^{k_1}[(k_1 + k_2)^{n-1} 2 \tau_0 s] + g_{n-1}^{k_2}[(k_1 + k_2)^{n-1} 2 \tau_0 s]\right\} \quad (30a)$$

$$\mu_1 = \tau\,, \quad \frac{\sigma_t^2}{\mu_1^2} = 2\gamma - 1 = \frac{(k_2 - k_1)^2}{(k_1 + k_2)(k_1 + k_2 - 2)} \quad (30b)$$

One checks that $\gamma = 1/2$ for $k_1 = k_2$ (identical paths in the two branches). When the difference $k_2 - k_1$ in the pathlengths is increased, figures 8a and b show that the RTDs are distorted, and can present several maxima. Such generating patterns would be interesting to model bypasses through fractured or heterogeneous media. In the limit $k_1/k_2 \to 0$, $E(t)$ is the sum of two equal Dirac peaks, one located at $t = 0$ corresponding to the by-pass through the volume $(k_1/(k_1 + k_2))\ V \to 0$, the other located at $t = 2\tau$, corresponding to the longest path through the volume $(k_2/(k_1 + k_2))\ V \to V$, crossed by a flowrate $Q/2$.

The shape of the RTD is very sensitive to the partition of the volumes in each channel. Figure 9 shows that for $k_1 + k_2 = 6$, and omitting the trivial case $k_1 = k_2 = 3$ leading to plug flow, the distribution with $k_1 = 1$, $k_2 = 5$ is very different from the distribution with $k_1 = 2$, $k_2 = 4$. In an equivalent manner, the shape of the RTD is also very sensitive to the partition of the flowrates in each channel. For $k_1 = 1$ and $k_2 = 2$, figure 10 shows the distortion of the RTD for various partitions, starting from the convergence condition $\omega_2 = 1/3$ which displays a monotically decreasing behavior without maximum.

These extreme situations clearly demonstrate that the first and second moments of $E(t)$, or the associated spatial moments, are not sufficient to depict dispersion properties of self-similar systems. In these particular cases, the computation of a dispersion coefficient would not make any sense. However, self-similar networks which present a narrow distribution of pathlengths in the generating pattern give rise to a « regular » RTD, with a single maximum (Fig. 7). In this case of anomalous (the diffusion front is not Gaussian), but « regular » dispersion (a single maximum), the RTD is fairly approximated by (16) and (29), at least for long times. The long time asymptotic form of the RTD may also be extracted from the generating pattern ; using Tauberian theorems [16], the asymptotic behavior of the limiting distributions is given by

$$E(t) \sim L(1/t)\, t^{-\rho} \quad \text{when} \quad t \to \infty$$

where $L(x)$ is a slow varying function at the origin (see Feller [16]), and ρ is the smallest root greater than 2 of

$$\sum_i \frac{k_i}{k} (k\omega_i)^{2-\rho} = 1\,.$$

4. Traps and dispersion by a stagnant phase.

For intermediate Péclet numbers, porous media are readily modelled by the fraction $1 - f$ of the volume where no hydrodynamic motion takes place [2, 3, 8]. The medium is assimilated to a network of convective paths (as previously) liable to exchange mass with a stagnant phase *via* essentially diffusive Brownian processes.

We want to sketch the incidence of a stagnant phase uniformly distributed into the volume. We assign a trap zone to each microscopic mixing cell in the network. Then, the basic element

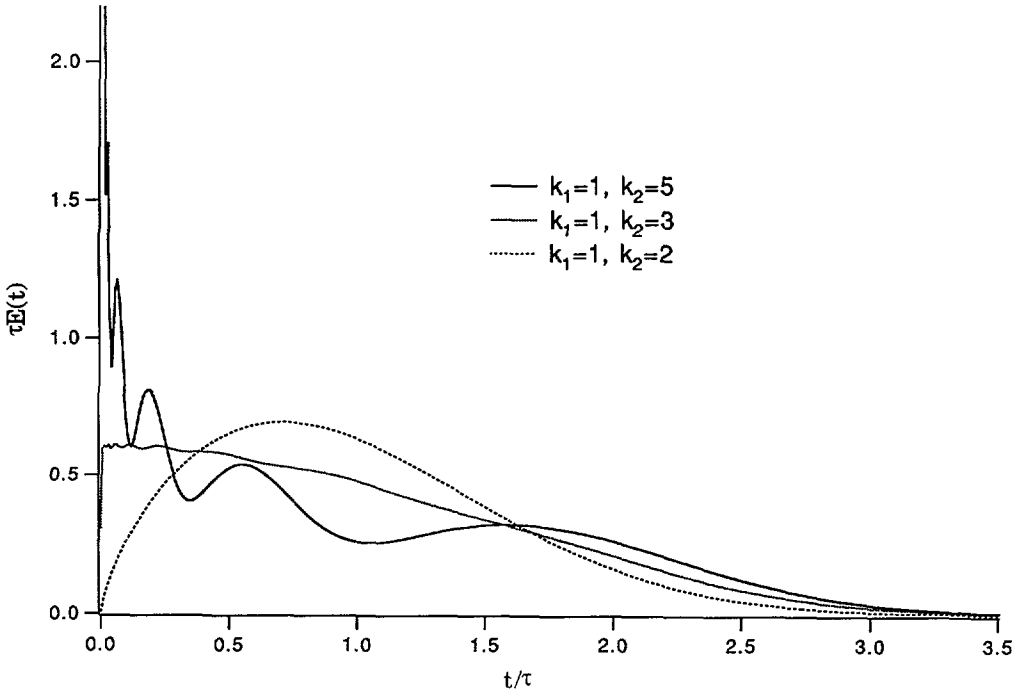

a)

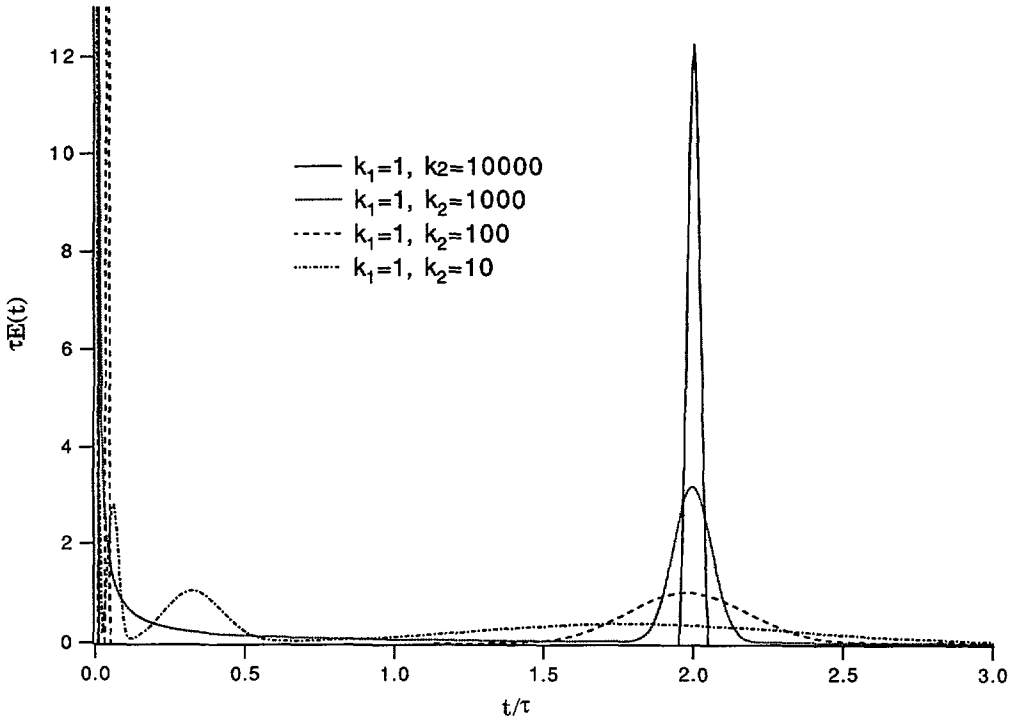

b)

Fig. 8. — RTD at generation $n = 50$ based on the generating patterns of figure 6b. Effect of increasing the difference in the pathlengths.

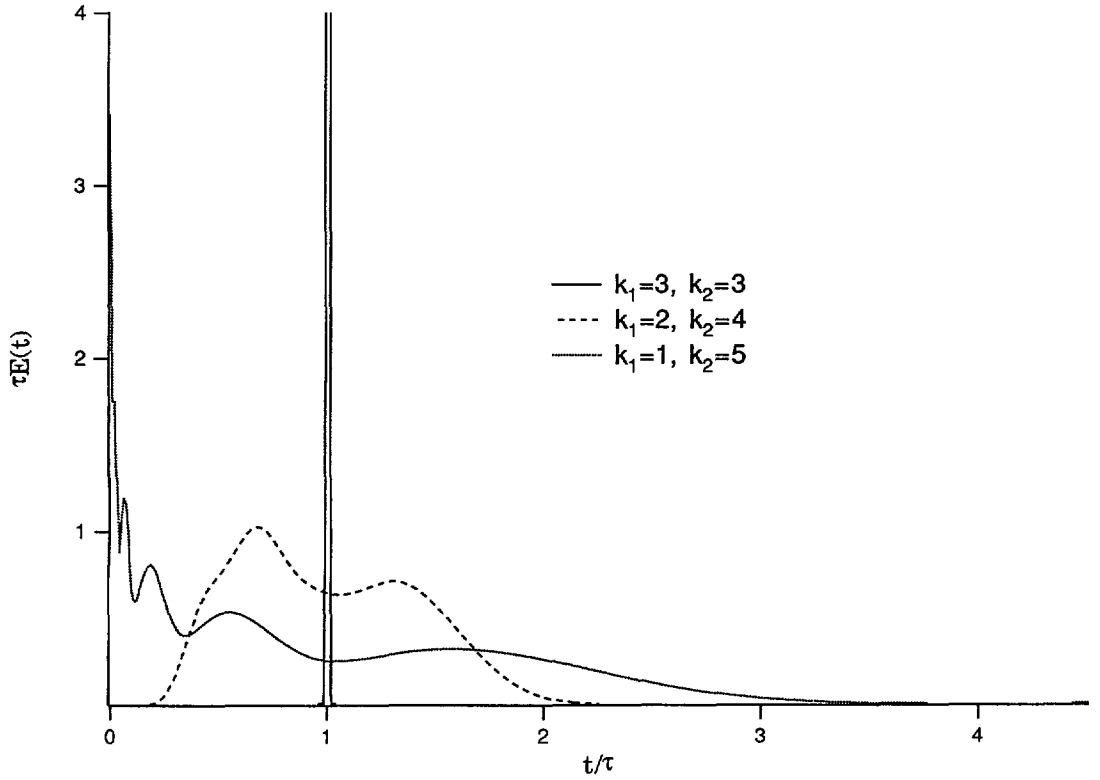

Fig. 9. — RTD at generation $n = 50$ based on the generating patterns of figure 6b with $k_1 + k_2 = 6$. Effect of the difference in the pathlengths.

of the network is divided in two subelements, first a convective path of volume fv_0, and second a stagnant zone of volume $(1 - f)\, v_0$ (Fig. 11). We assume that these zones are coupled by a first order mass transfer law of the form

$$\frac{dC_s}{dt} = \frac{C_0 - C_s}{t_m} \tag{31}$$

where C_s and C_0 are the concentrations of tracer in the stagnant zone and in the convective path respectively, and t_m is a characteristic hold-up time. This law is equivalent to an exponential release contribution of the tracer at each step [3, 13, 14].

Linear adsorption could easily be embedded in (31) by replacing $C_0 - C_s$ by $C_0/K - C_s$, K being an equilibrium partition coefficient depending on temperature. The trapping time t_m depends on the detailed mechanism of the transfer process, and it can be interpreted either as the exploration time of some small scale ℓ of the medium ($t_m = \ell^2/D_m$ or ℓ^2/D_a, D_a beeing the « ant » diffusion constant defined by [1] when ℓ is a fractal lengthscale), or as the characteristic desorption time constant of an adsorption process [1, 2]. An elementary mass balance gives the transfer function of the microscopic cell (Fig. 11)

$$g_0(\tau_0 s, t_m) = \frac{1}{1 + f\tau_0 s + \dfrac{(1-f)\,\tau_0 s}{1 + t_m s}} \tag{32}$$

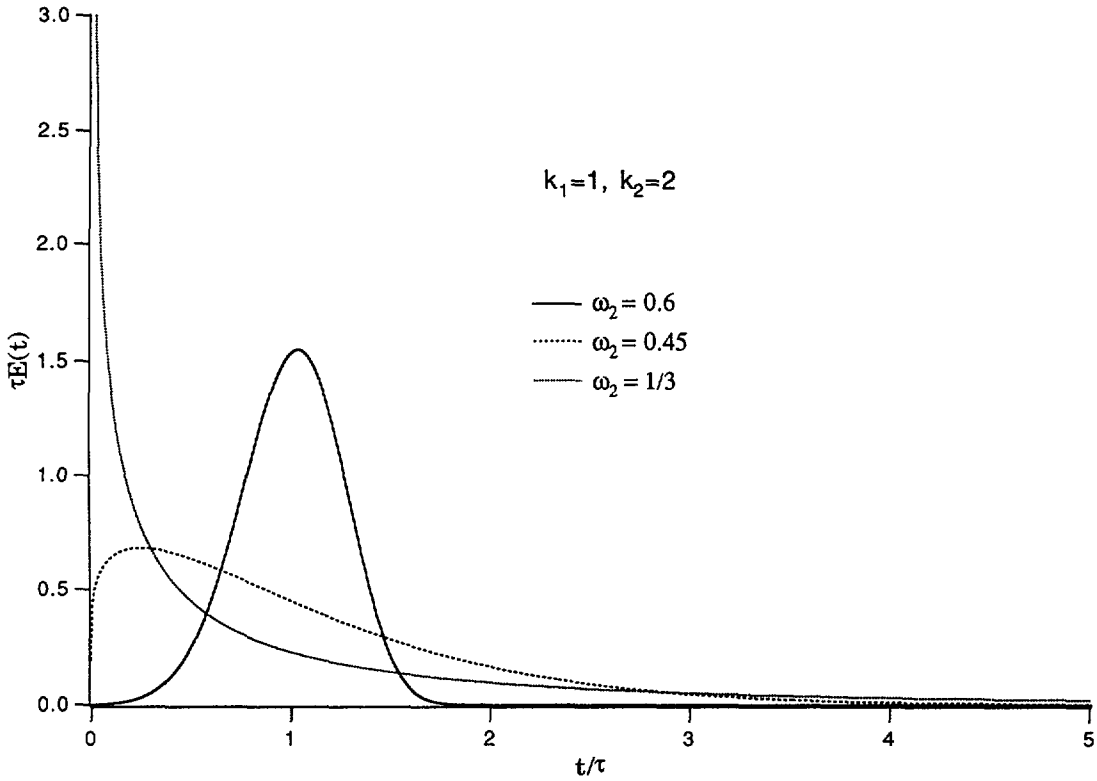

Fig. 10. — RTD at generation $n = 10$ based on the generating patterns of figure 6b with $k_1 = 1$, $k_2 = 2$. Effect of flowrate splitting, ω_2 is chosen to ensure moments convergence.

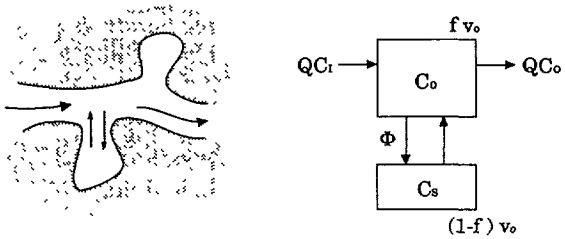

Fig. 11. — Left : stagnation zone adjacent to a pore in the actual medium. Right : trapping is accounted for by a microscopic volume v_0 which is divided into a convective fraction fv_0, and a stagnant fraction $(1 - f)\, v_0$. The two fractions are coupled by a first order mass transfer law.

The limiting situations where $f = 1$ or $t_m = 0$ restore the previous microscopic function (14). If t_m scales as τ_0 ($t_m = \lambda \tau_0$, λ = constant), then $g_0(\tau_0 s, t_m)$ becomes a function of $\tau_0 s$ only as in the absence of stagnation effect. The results of section 3 hold and the limiting RTD is independent of the trapping phenomenon. This is easily understood since in that case the traps are vanishingly small at infinite generation. If t_m is related to a process that does not

follow a scaling law (t_m independent of n), equations (20), (21) still hold, whereas the second order expansion of g_0 is

$$g_0(\tau_0 s, t_m) = 1 - \tau_0 s + (2(1-f)\tau_0 t_m + \tau_0^2)\frac{s^2}{2} + O(s^3) . \tag{33}$$

The term $2(1-f)\tau_0 t_m$ accounting for stagnation effects is linear in τ_0, and thus it renormalizes like the first order moment $\mu_{1,n} = \tau$ to become $2(1-f)\tau t_m$ at the n-th generation. Furthermore, we know that flow and trapping effects additively contribute to the variance of the RTD [9]. Consequently, the expansion of the transfer function is

$$G_n(s) = 1 - \tau s + [\gamma_n \tau^2 + (1-f)\tau t_m] s^2 + O(s^3) \tag{34}$$

where γ_n is still given by (25), and convergence of moments is ensured by (21b). The limiting variance is thus composed of two terms

$$\sigma_t^2 = (2\gamma - 1)\tau^2 + 2(1-f)\tau t_m . \tag{35}$$

The first corresponds to the previously discussed geometrical dispersion contribution, and the second accounts for stagnation effects which, as expected, vanish for $f = 1$ or $t_m = 0$.

5. The dispersion coefficient.

When this coefficient makes sense (i.e., essentially when the distribution $E(t)$ has only one maximum), the expression for the dispersion coefficient in a linear sample of size L can be derived as explained below. We assume that the medium is locally self-similar over a correlation length ξ, and we picture the medium as a series of $P = L/\xi$ fractal elements or blobs (Fig. 12). Consequently, if $G(s)$ is the transfer function of the self-similar element, then the transfer function, $G_P(s)$ of the whole system is

$$G_P(s) = [G(s)]^P \tag{36}$$

The mean square spatial deviation of the tracer distribution is

$$\sigma_x^2 = \langle x^2 \rangle - \langle x \rangle^2 = 2 D_\parallel \mu_1 \tag{37a}$$

$$\sigma_x^2 = U^2(\mu_2 - \mu_1^2) = U^2 \sigma_t^2 \tag{37b}$$

then, $D_\parallel$ reads, as a function of the variance of the residence time distribution

$$D_\parallel = \frac{U^2}{2}\frac{\sigma_t^2}{\mu_1} \tag{38}$$

The variance σ_t^2 is derived from the whole transfer function of the sample in its expanded form (34)

$$G_P(s) = \left\{1 - \left(\frac{\tau}{P}\right) s + \left[\gamma\left(\frac{\tau}{P}\right)^2 + (1-f)\frac{\tau}{P} t_m\right] s^2 + O(s^3)\right\}^P \tag{39}$$

where $\tau = \mu_1 = V/Q = L/U$, and $P = L/\xi$. From (8), one finds $\sigma_t^2 = (2\gamma - 1)\tau^2/P + 2(1-f)\tau t_m$ and

$$D_\parallel = \left(\gamma - \frac{1}{2}\right) U\xi + (1-f) U^2 t_m . \tag{40}$$

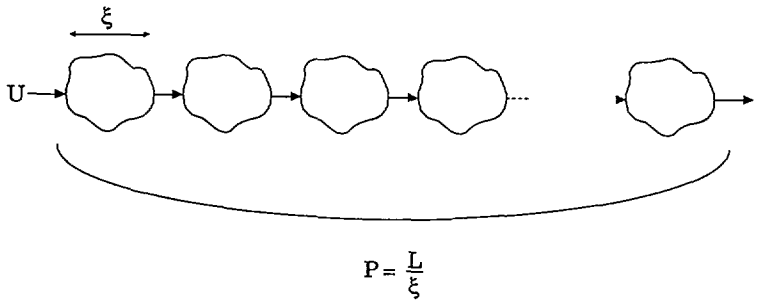

Fig. 12. — A disordered medium is modeled by a series of P fractal cells of size equal to the correlation length ξ.

The dependence $D_{\parallel} \sim U\ell_d$ is characteristic of geometric dispersion [3, 8]. Here, the dispersion length $\ell_d = (\gamma - 1/2)\,\xi$ is a fraction of the correlation length ξ. The contribution to $D_{\parallel}$ of stagnation is proportional to U^2, which is characteristic of trapping. One may notice that dispersion can occur without geometrical effects ($\gamma = 1/2$), as commonly encountered in linear chromatography for instance [9].

Concluding remarks.

Our model is based on the microscopic principle of continuity and applies to disordered media bearing a local self-similarity. The fractality is not an essential feature of the resulting dispersion process since no fractal dimension emerges from our computations. Only the connectivity of the network plays a major role *via* the difference of pathlengths in the generating pattern.

The self-similarity roughly results in two contrasting situations. When the distribution of pathlengths in the generating pattern is narrow, the RTD has a single maximum and it looks like the RTD of a standard dispersed plug flow. We call « regular dispersion » this situation where the definition of a dispersion coefficient makes sense, and where the dispersion coefficient splits in two additive contributions (i.e., geometrical and trapping) as already known [1, 3, 10-12].

When the distribution of pathlengths in the generating pattern is broad, the existence of bypasses through the macroscopic fractal region is revealed by a RTD with several maxima. We call this situation « irregular dispersion ». In this case the definition of a dispersion coefficient does not make any sense since the first two time-moments are not sufficient to characterize the RTD. We strongly emphasize that the dispersion front is never Gaussian in spatial dimensions.

Standard flow models, based on mass balance equations, lead either to ordinary differential equations (see Eq. (13)) or to partial differential equations (see Eqs. (1) and (2)). In the Laplace domain, $G(s)$ is thus defined either by an algebraic equation or by a differential equation which is generally easy to solve. On the contrary, self-similarity results in an implicit fixed point equation for $G(s)$ (see Eq. (20b)), which is generally impossible to solve explicitly. It would be interesting to study the properties of these equations in order to get some general results relating the RTD to the structure of the generating pattern. Unfortunately, it seems that there is no simple method for deriving the fixed point equation from a visual inspection of the generating pattern, except in very simple cases as those dealt with in this paper.

We have assumed that the basic element of the generating pattern is defined by a single transfer function $g_0(\tau_0 s)$, and we have shown that the limiting RTD is in dependent of g_0 for any pattern composed of parallel branches with a flow partition which ensures moments convergence. It would be interesting to know whether the RTD converges towards a unique limit $E(t)$ independent of g_0 for large n in case of diverging moments. More general situations where the generating pattern is composed of different basic elements (multifractal sets) could also be studied. Do these systems exhibit a more « regular » dispersion behavior (smoother RTD) or a more « irregular » one (more randomly located peaks than those of Fig. 8) ? In case of « irregular dispersion », one may wonder whether there exist some generating pattern which could lead to a RTD composed of a « chaotic » series of peaks. The latter situation would probably be a candidate for modeling turbulent dispersion and flows where large scale eddies induce more or less random peaks in the early stage of a RTD.

Acknowledgments.

Dr. J. P. Hulin is gratefully acknowledged for useful discussions and criticisms. E. Villermaux wishes to thank the Laboratoire d'Aérothermique du CNRS (Meudon, France), where part of this work was done, for its hospitality.

Appendix.

Consider a generating pattern made of i parallel branches, each of them being composed of k_i identical cells in series and crossed by a fraction ω_i of the total flowrate Q (Fig. 13). We assume that there is no stagnation effect in the elementary cell. The transfer function $G_n(s)$ of the network at the n-th generation is given as a function of the transfer function of the previous generation g_{n-1} by the recurrence relation (Same derivation as in the example of Fig. 4 ; see Sect. 3)

$$G_n(s) = g_n(\tau s) = \sum_i \omega_i \left(g_{n-1}\left[\frac{\tau s}{k\omega_i} \right] \right)^{k_i} \tag{A1}$$

with

$$k = \sum_i k_i , \qquad \sum_i \omega_i = 1 \tag{A2}$$

$$\tau = k^n \tau_0 . \tag{A3}$$

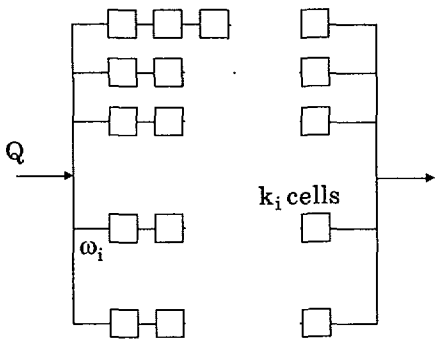

Fig. 13. — General generating pattern made of i parallel branches bearing k_i cells each and fed by the fraction ω_i of the inlet flowrate Q.

At each generation n, the macroscale (i.e. τ) is defined from the microscale (i.e. τ_0) by the dilatation factor k^n, where k is the total number of cells in the generating pattern. Let $G_n^{(j)}(s)$ be the derivative of $G_n(s)$ with respect to s and let $\mu_{j,n}$ be the moment of order j of $G_n(s)$. According to (7), one has

$$G_n^{(j)}(s) = \tau^j g_n^{(j)}(\tau s) \quad \text{and} \quad \mu_{j,n} = (-1)^j \tau^j g_n^{(j)}(0) . \tag{A4}$$

With the following properties, holding for any microscopic transfer function

$$g_0(0) = 1 ; \quad \left(\frac{\mathrm{d}g_0(\tau s)}{\mathrm{d}s} \right)_{s=0} = -\tau = \tau g'(0) \quad \text{thus} \quad g'(0) = -1 . \tag{A5}$$

With $x = \tau s$ and $x_i = x/k\omega_i$, one computes all the moments $\mu_{j,n}$ by successive derivations of (A1).

Order 0 :

$$g_n(0) = 1 \quad \text{by direct recurrence with} \quad g_0(0) = 1 \tag{A6}$$

$$G(0) = 1 . \tag{A7}$$

Order 1 :

$$g_n'(x) = \sum_i \frac{k_i}{k} (g_{n-1}(x_i))^{k_i - 1} g_{n-1}'(x_i) \tag{A8}$$

$$g_n'(0) = g_{n-1}'(0) = g_0'(0) = -1 \tag{A9}$$

$$\mu_{1,n} = \tau . \tag{A10}$$

Order 2 :

$$g_n''(x) = \sum_i \frac{k_i}{k^2 \omega_i} [(k_i - 1)(g_{n-1}(x_i))^{k_i - 2} g_{n-1}'^2(x_i) + (g_{n-1}(x_i))^{k_i - 1} g_{n-1}''(x_i)] \tag{A11}$$

$$g_n''(0) = \sum_i \frac{k_i}{k^2 \omega_i} [(k_i - 1) + g_{n-1}''(0)] . \tag{A12}$$

Let

$$A = \sum_i \frac{k_i}{k^2 \omega_i} , \qquad B = \sum_i \frac{k_i(k_i - 1)}{2 k^2 \omega_i} \tag{A13}$$

The recurrence for the moments is then

$$\mu_{2,n} = 2 B \tau^2 + A \mu_{2,n-1} . \tag{A14}$$

Looking for an expansion of the type

$$g_n(x) \approx 1 - x + \gamma_n x^2 \tag{A15}$$

one obtains

$$\gamma_n = B + A \gamma_{n-1} \tag{A16}$$

that is to say

$$\gamma_n = \frac{A^n g_0''(0)}{2} + B \frac{1 - A^n}{1 - A} \tag{A17}$$

If $A = 1$, γ_n diverges with n such that

$$\gamma_n = 1 + nB . \tag{A18}$$

When $A < 1$, γ_n goes to the limit γ

$$\gamma = \frac{B}{1 - A} . \tag{A19}$$

The variance of the distribution is then given by

$$\frac{\sigma_t^2}{\tau^2} = 2\,\gamma - 1 . \tag{A20}$$

Remarks :

1) If $k\omega_i > 1$ for any i, then

$$A = \sum_i \frac{k_i}{k^2\,\omega_i} < \sum_i \frac{k_i}{k} = 1 .$$

In this case, the variance σ_t^2 and γ remain bounded.

2) The variance is zero if $\gamma = 1/2$ (plus flow), giving also

$$k^2 = \sum_i \frac{k_i^2}{\omega_i}$$

Order 3 :

$$g_n'''(x) = \sum_i \frac{k_i}{k^3\,\omega_i^2} [(k_i - 1)(k_i - 2)\, g_{n-1}(x_i)^{k_i - 3}\, g_{n-1}'^3(x_i) + \\ + 3(k_i - 1)\, g_{n-1}(x_i)^{k_i - 2}\, g_{n-1}''(x_i) + g_{n-1}(x_i)^{k_i - 1}\, g_{n-1}'''(x_i)] \tag{A21}$$

$$g_n'''(0) = \sum_i \frac{k_i}{k^3\,\omega_i^2} [g_{n-1}'''(0) - (k_i - 1)(k_i - 2) - 3(k_i - 1)\, g_{n-1}''(0)] \tag{A22}$$

$$\mu_{3,n} = \mu_{3,n-1}\left(\sum_i \frac{k_i}{k^3\,\omega_i^2}\right) + 3\,\tau\mu_{2,n-1}\left(\sum_i \frac{k_i(k_i - 1)}{k^3\,\omega_i^2}\right) + \tau^3\left(\sum_i \frac{k_i(k_i - 1)(k_i - 2)}{k^3\,\omega_i^2}\right) . \tag{A23}$$

Order j :

$$g_n^{(j)}(x) = \left(\sum_i \frac{k_i}{(k\omega_i)^{j-1}} \frac{g_{n-1}^{(j)}(x_i)}{k}\, g_n(x_i)^{k_i - 1}\right) + g_{n-1}^{(j-1)}(x_i) .. \tag{A24}$$

$$\mu_{j,n} = \frac{\mu_{j,n-1}}{k}\left(\sum_i \frac{k_i}{(k\omega_i)^{j-1}}\right) + \mu_{j-1,n-1} \cdot = \mu_{j,n-1}\, C_j + \cdot \tag{A25}$$

The moment $\mu_{j,n}$ is proportional to the moment of the same order j of the previous generation $n - 1$ *via* coefficient C_j plus a contribution of the moments of order lower than j with

$$C_j = \sum_i \frac{k_i}{k} \frac{1}{(k\omega_i)^{j-1}}, \quad C_2 = A . \tag{A26}$$

From (A25), the moment $\mu_{j,n}$ converges with n if and only if all the lower moments converge and $C_j < 1$. If there exists one branch for which $k\omega_i < 1$, then $\mu_{j,n}$ will start to diverge with n as soon as j reaches j^* such that $1/(k\omega_i)^{j^*-1}$ makes C_j to become greater than 1. Conversely, if $\mu_{j,n}$ converges at any order j, then $C_j < 1$ for any j and all the moments of order lower than j converge. The conclusion is then that all the moments of the distribution $G_n(s)$ converge if and only if

$$k\omega_i > 1 . \tag{A27}$$

Particular choices of the distribution of ω_i .

1) Equipartition of the flowrate Q in N branches. — Then $\omega_i = 1/N$ and $k \geqslant N$. Consequently, condition (A27) is always fulfilled, the equality $k\omega_i = 1$ corresponding to the case where all branches are composed of a unique elementary cell, (1) leading to $g_n = g_{n-1} = g_0$.

2) Partition of ω_i with equal pressure drop in all branches. — If the flowrate admitted in each branch bearing k_i cells is such that the pressure drop (or voltage) is the same for each branch, then $k_i\,\omega_i$ must be a constant independent of i. This gives

$$\omega_i = \frac{1}{k_i \sum_j \frac{1}{k_j}} . \tag{A28}$$

One checks that for all $k_j \geqslant 1$, $\Sigma k_j \geqslant k_i\ \Sigma 1/k_j$, then for all i, $k\omega_i = \omega_i\ \Sigma k_j \geqslant 1$, and all the moments of $G_n(s)$ converge with n.

An infinite series of bounded moments uniquely defines a Laplace transform [16]. Consequently, when $\mu_{j,n}$ converges with n, the existence and uniqueness of a limit $G(s)$ to the solution of the recurrence equation (A1) is demonstrated. Moreover, since C_j and $\mu_1 = \tau$ are independent of g_0, the series of limiting moments and $G(s)$ are also independent of g_0. It is thus necessarily the unique solution of the fixed point equation

$$G(s) = g(\tau s) = \sum_i \omega_i \left(g\left[\frac{\tau s}{k\omega_i} \right] \right)^{k_i} \tag{A29}$$

This also demonstrates that the final distribution function and its moments (especially γ) are unsensitive to the details of the microscopic elementary cell (i.e. g_0) and that only the connections inside the hierarchical structure (k_i, ω_i) play a role at the macroscale.

References

[1] DE GENNES P. G., *J. Fluid Mech.* **136** (1983) 189-200.

[2] SCHWEICH D., Disorder and Mixing, E. Guyon *et al.* Eds. (Kluwer Academic Publishers, 1988) pp. 57-84.

[3] BACRI J. C., BOUCHAUD J. P., GEORGES A., GUYON E., HULIN J. P., RAKOTOMALALA N. and SALIN D., in Proceedings of the 4th EPS Conference on the Hydrodynamics of Dispersed Media, (1989) and ;

BOUCHAUD J. P. and GEORGES A., *Phys. Rep.* 195, n 4 & 5 (1990).

[4] SAHIMI M., GAVALAS G. R. and TSOTSIS T. T., *Chem. Eng. Sci.* **45** (1990) 1443-1502.

[5] DANCKWERTS P. V., *Chem. Eng. Sci.* **2** (1953) 1.

[6] VILLERMAUX J., Génie de la réaction chimique (Lavoisier Ed, 2nd Edition, Paris, 1985).
[7] WEN C. Y. and FAN L. T., Models for Flow Systems and Chemical Reactors, M. Dekker Ed. (1975).
[8] FRIED J. J. and COMBARNOUS M., *Adv. Hydrosci.* **7** (1971) 169.
[9] VILLERMAUX J., Theory of Linear Chromatography, in Percolation Processes, NATO advanced studies institute E33, Eds. Sijtoff and NoordHoff (1981).
[10] KOCH D. L. and BRADY J. F., *J. Fluid Mech.* **154** (1985) 399-427.
[11] KOPLIK J., REDNER S. and WILKINSON D., *Phys. Rev. A* **37** (1988) 7.
[12] GIST G. A., THOMPSON A. H., KATZ A. J. and HIGGINS R. L., *Phys. Fluids A* **2** (1990) 9.
[13] MONTROLL E. W. and WEISS G. H., *J. Math. Phys.* **6** (1965) 167-181.
[14] HUGHES B. D. and PRAGER S., Random processes and random systems, in The mathematics and physics of disordered media (Springer Verlag) *Lecture Notes in Mathematics* (1983) p. 1035.
[15] CLERC J. P., GIRAUD G., LAUGIER J. M. and LUCK J. M., *Adv. Phys.* **39** (1990) 191-309.
[16] FELLER, An Introduction to Probability Theory and its Applications (Wiley, 2nd edition, 1966).